Product branching ratios in the reaction of Xe*(3 P 2,0) with IBr. Role of excited potential surface

Mattanjah S. de Vries, George W. Tyndall, and Richard M. Martin

Citation: The Journal of Chemical Physics **81**, 2352 (1984); doi: 10.1063/1.447934
View online: http://dx.doi.org/10.1063/1.447934
View Table of Contents: http://scitation.aip.org/content/aip/journal/jcp/81/5?ver=pdfcov
Published by the AIP Publishing

Product branching ratios in the reaction of $Xe^*(^3P_{2,0})$ with IBr. Role of excited potential surface

Mattanjah S. de Vries, George W. Tyndall, and Richard M. Martin
Department of Chemistry, University of California, Santa Barbara, California 93106

(Received 15 August 1983; accepted 20 March 1984)

The reaction of $Xe^*(^3P_{2,0})$ with IBr to form the XeI* and XeBr* excimers was studied using two crossed molecular beam techniques. Emission spectra were obtained between 200 and 400 nm, and relative cross sections and branching ratios were measured as a function of collision energy over the range 15–420 meV. The observed effects are discussed in terms of a curve crossing model, involving the neutral potential surface and both ground and excited $Xe^+ + IBr^-$ potential surfaces. In this model, XeBr* is formed from the ground state ionic potential and XeI* is formed from the excited potential.

I. INTRODUCTION

Collisions of metastable rare gas atoms (A*) with diatomic halogen molecules (XY) are characterized by a long range curve crossing.[1–3] These systems are analogous to the much studied alkali/halogen systems.[2] A metastable rare gas atom can be regarded as an alkali atom with a core hole, which does not seem to have much influence on the collision dynamics, especially at long range. Several studies have pointed to the common characteristics of these types of collisions.[3–5] However the internal energy that is carried by the metastable rare gas atoms opens the way to reaction mechanisms which are absent with the alkali/halogen systems, e.g., Penning ionization and excitation transfer. Both of these processes have been studied in flowing afterglow experiments as well as with molecular beams.[6] A practical aspect of the electronic excitation of the metastable in reaction dynamics studies is that the reaction products may be formed in an excited electronic state. This makes them well suited for studying the behavior of different reaction channels by detection of the chemiluminescence at different wavelengths. We have recently made use of this to study the competition between excitaton transfer and atom transfer reactions in A^*/X_2 collisions, by distinguishing between X_2^* and AX* emission.[7] Another important question arises with A*/XY collisions, concerning the formation of AX* vs AY*. As will be discussed below, an excited intermediate potential surface is thought to play a role in the formation of one of the products. With homonuclear X_2 reactions the different potential surfaces lead to the same product, but there is evidence from studies of the spectra that the excited potential surface is also involved in these reactions.[3,8] With the alkali/XY systems both MX and MY are produced, but there is little information available about their branching ratios.

In the present paper we report on a study of the branching ratio for the reactions:

$$Xe(^3P_{2,0}) + IBr \rightarrow XeI^* + Br \quad (1a)$$

$$\rightarrow XeBr^* + I. \quad (1b)$$

The chemiluminescence spectrum from XeI* and XeBr* emission was measured, and product branching ratios were obtained as a function of collision velocity.

II. EXPERIMENTAL

Two crossed molecular beam machines were used in the present work, one for chemiluminescence spectroscopy and the other for time-of-flight (TOF) translational spectroscopy. The chemiluminescence spectra were measured in a slightly modified version of an apparatus that has previously been described.[9] A rare gas nozzle beam passed through a Penning ionization discharge in which metastables were formed.[10] Ions and Rydberg states were removed by sweeper plates downstream. The Xe* nozzle beam was crossed by an effusive IBr beam, which was collimated by a liquid nitrogen cooled cold shield. Chemiluminescence, emitted from the interaction region, is collected by a quartz lens and focused onto the entrance slit of a $f/5.3$ monochromator. The light was detected by a cooled photomultiplier tube using photon counting techniques. The monochromator was stepped through the spectrum under computer control, collecting data at each wavelength for a preset time. In order to correct for long term drifts in beam intensities, a second photomultiplier simultaneously monitored the total (undispersed) chemiluminescence. The IBr beam was periodically chopped with a beam flag to allow for subtraction of background radiation, mainly due to collisions of Xe* with residual gas. The spectral response function of the optical system was determined over the 200–400 nm region using a deuterium standard lamp. The time-of-flight apparatus has been described in detail elsewhere.[7,11] The Xe* source was similar to that in the chemiluminescence spectroscopy apparatus, except that an effusive Xe beam was used to obtain a broad velocity distribution. The Xe beam was chopped by a pulser wheel for time-of-flight velocity separation, and crossed by an effusive IBr beam after a flight path of 30 cm. Metastables were detected by impinging on a Ta grid, causing electron emission which was measured by pulse counting using a channel electron multiplier. Photons, emitted in the interaction region, were detected by a photomultiplier tube. By simultaneously detecting metastables and photons as a function of flight time the relative chemiluminescence cross section can be obtained as a function of collision velocity. Various parts of the chemiluminescence spectrum can be isolated by inserting filters in front of the photomultiplier tube, which permits the

 0021-9606/84/172352-05$02.10

TOF study of different reaction channels in favorable cases.

The IBr beam was chopped with a beam flag to provide for background subtraction, and TOF spectra were recorded using a home built interface to a minicomputer.

III. RESULTS

A. Chemiluminescence spectra

Figure 1 shows a spectrum obtained from Xe* + IBr with both beams at room temperature, giving an average collision energy of about 40 meV. The spectrum consists of overlapping emission from both XeI* and XeBr*. For comparison, Fig. 2 shows the spectra that we obtained when IBr was replaced with Br_2 and I_2, respectively. All spectra were taken at the same beam temperatures and pressures. The assignment of the peaks follows that by Setser *et al.*[3,8] based on the potentials by Hay and Dunning.[12] The spectrum of Xe*/IBr consists of six contributions, namely, the (*B-A*), (*B-X*), and (*C-A*) emission bands of the two excimers. The composite spectrum of Fig. 1 was obtained from the Xe*/Br_2, I_2 spectra of Fig. 2. The best fit to the Xe*/IBr spectrum was obtained by varying the relative contributions of the Xe*/Br_2 and Xe*/I_2 spectra, as well as the ratio of *B* state to *C* state emission within each spectrum. We find that the XeI* from IBr is formed with a somewhat smaller electronic state *C*/*B* branching ratio than from I_2. On the other hand, the *C*/*B* ratio of XeBr* from IBr is two and a half times that of XeBr* formed from Br_2. We estimate the XeI*/XeBr* branching ratio from IBr to be 0.40. These results are based on the assumption that the excimers from Xe*/Br_2, I_2 have the same rovibronic distribution as those from Xe*/IBr. The composite spectrum is not sensitive to this assumption, since these are bound-free spectra giving continuum emission.

Electron bombardment excitation in the 80–160 eV region has been found to produce the statistical $^3P_2/^3P_0$ ratio of

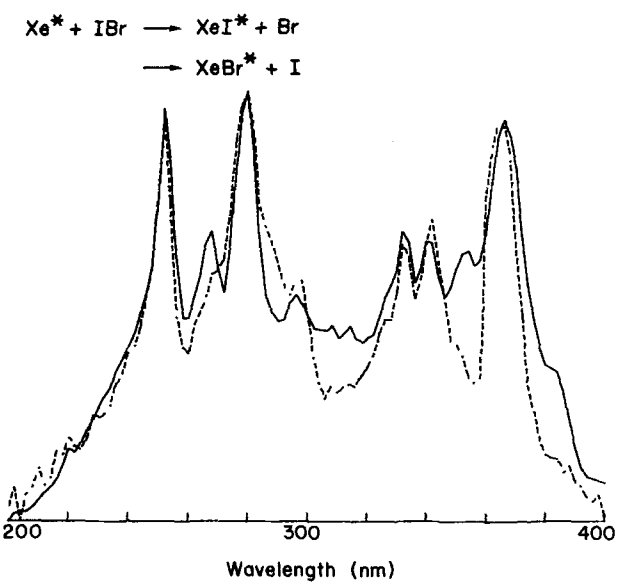

FIG. 1. XeBr* and XeI* emission spectrum from the reaction of Xe* with IBr at 40 meV collision energy. The solid line is the experimental spectrum corrected for apparatus spectral response, and the dashed line is the composite spectrum from convolution of the spectra in Fig. 2, as described in the text.

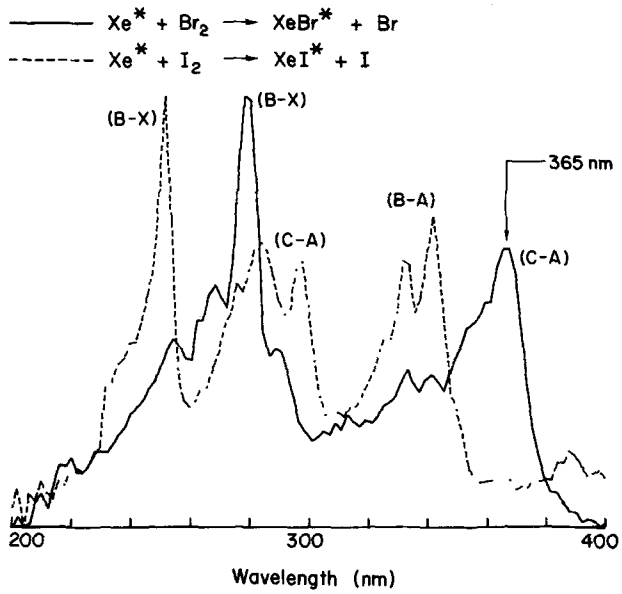

FIG. 2. XeBr* spectrum from reaction of Xe* with Br_2 (solid line) and XeI* spectrum from reaction of Xe* with I_2 (dashed line). Experimental conditions were the same as for Fig. 1.

5 in neon.[13] However the conditions of the source used in the present work (i.e., a magnetically collimated high voltage discharge) could give a much different ratio. The absence of *D* state excimer emission in our experiments suggests the absence of Xe($^3P_0$) in our beam, because the $^3P_0$ state correlates with the *D* state, through the $Xe^+(^2P_{1/2})$ ionic intermediate. The excimers are formed by a crossing from the A* + XY neutral potential to a $A^+ + XY^-$ ionic potential. The A^+ then combines with the negative halogen ion (X^- or Y^-) to form the excimer. Removing the outer (*s*) electron from A($^3P_0$) produces $A^+(^2P_{1/2})$, while removing the *s* electron from A($^3P_2$) produces $A^+(^2P_{3/2})$. As a result, assuming that two electron rearrangements are unlikely, we can predict which intermediate ionic potential surface will be followed by each of the metastable states. The AX* D state correlates with $A^+(^2P_{1/2}) + X^-$, while the *B* and *C* states correlate with $A^+(^2P_{3/2}) + X^-$. Combined with the absence of *D* state emission, this indicates that the observed excimer states were formed mainly from Xe($^3P_2$) reactions. This is consistent with the results of Setser and co-workers from flowing afterglow experiments. They found only minor amounts of XeI(*D*) and XeBr(D) emission from reactions of diatomic halogens.[3,8] The Xe($^3P_0$) concentration was below the detection limit of absorption spectroscopy,[14] and no evidence for the $^3P_0$ state was found from the short wavelength limit of the XeCl* spectrum from Xe* + Cl_2,[14] or from the emission spectra of Xe* + N_2.[15]

B. Cross section velocity dependence

Figure 3 shows a double logarithmic plot of the relative chemiluminescence cross section as a function of relative velocity. The radiation was detected using a Corning 7-54 filter coated with 1 mg/cm^2 of sodium salicilate,[16] in front of the photomultiplier. This coating fluoresces in the 400–500 nm region with a constant quantum yield of 0.5 over the

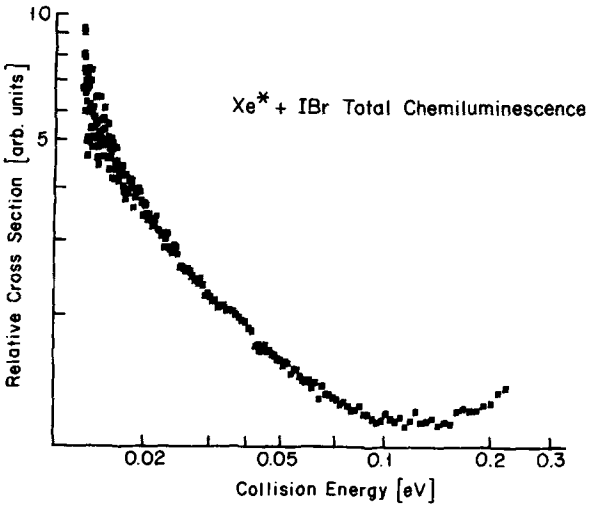

FIG. 3. Logarithmic plot of relative total chemiluminescence vs collision energy for Xe* + IBr.

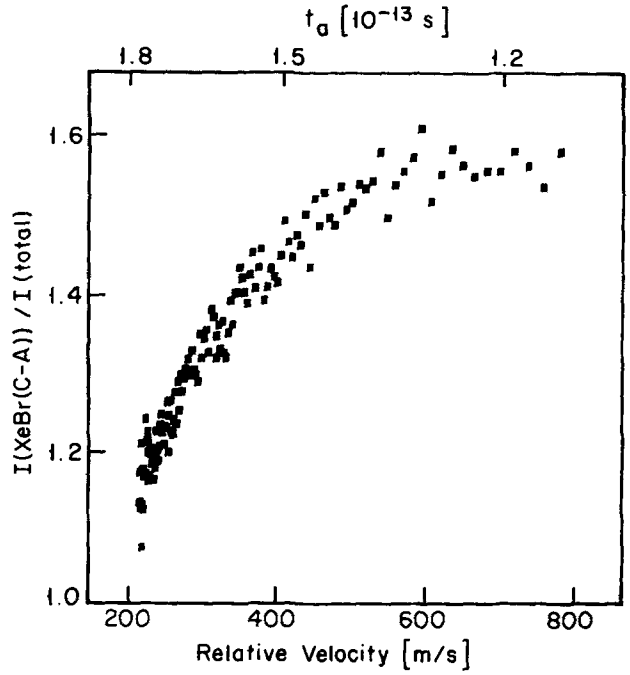

FIG. 4. Relative XeBr* (*C-A*) emission as a function of relative velocity. The top scale shows the time t_a as explained in text.

entire wavelength region of the Xe*/IBr chemiluminescence spectrum. Therefore variations in branching ratios as a function of velocity do not affect the measurement of the total chemilumenescence cross section. We have previously found that metastable rare gas/halogen total chemiluminescence cross sections are governed by an orbiting controlled harpoon mechanism.[7] The same general behavior has been reported by Rettner and Simons for Xe* + Br_2 collisions.[17] In this model[18] each trajectory that reaches an internuclear distance R_c experiences an electron jump. After this the trajectory follows the ionic potential surface and proceeds to reaction with unit probability. R_c is the curve crossing distance between the incoming neutral curve and the ionic curve, given by $R_c = e^2/\Delta V$, where ΔV is the difference between the ionization potential (I.P.) of the metastable and the electron affinity (E.A.) of the halogen molecule. If the incoming potential is given by C/R^s, the trajectories have to pass a centrifugal barrier in order to reach R_c. The position of that barrier depends upon the translational energy E, i.e., the barrier is at R_c when the energy equals E'[19]:

$$E' = (s-2)\frac{C}{2R_c s}. \tag{2}$$

When $E < E'$ the centrifugal barrier is outside R_c, and the orbiting cross section can be written as

$$\sigma = \frac{s\pi}{s-2} R_c^2 \left(\frac{E'}{E}\right)^{2/s}, \quad (E < E'). \tag{3}$$

For $E > E'$ the barrier is inside R_c and the cross section is given by

$$\sigma = \pi\left(1 + \frac{2E'}{(s-2)E}\right) R_c^2, \quad (E > E'). \tag{4}$$

From Eqs. (3) and (4) it is expected that a plot of ln σ vs ln E will give a straight line with slope $-2/s$ up to $E = E'$, and will level off for $E > E'$. This prediction is followed very well by the Ar*,Kr*/Cl_2,Br_2 total chemiluminescence cross sections.[7] As shown in Fig. 3, this behavior is also followed qualitatively by Xe* + IBr, but the quantitative agreement is not very good. We find $s \sim 4.5$ at low collision energies, significantly less than the value of 6 expected for the long range van der Waals potential. It is difficult to assign a unique value to E', and the slight increase in signal at higher energies is also not predicted by Eqs. (3) and (4). The model may have to be refined by using adiabatic potentials, and by considering a second curve crossing as will be discussed below.

It is difficult to detemine the velocity dependence of the product branching ratios, because the spectra of the different products are strongly overlapped (Fig. 1). Only the XeBr* *C-A* state emission between 350 and 380 nm is fairly unique. We have used a 10 nm bandwidth interference filter centered around 365 nm to isolate this emission. Figure 4 shows the relative branching ratio for this emission ($\sigma_{365\,nm}/\sigma_{total}$) as a function of collision velocity. Assuming that the XeBr *B/C* branching ratio is not velocity dependent, this is a measure of the relative $\sigma_{XeBr^*}/\sigma_{total}$ branching ratio as a function of velocity.

IV. DISCUSSION

The problem of product branching ratios has received attention with the analogous alkali/halogen reactions, because it is thought to involve an excited intermediate potential surface.[19] Figure 5 shows schematically the relevant IBr potentials. The potentials indicate that ground state IBr^- dissociates into I + Br^-, while IBr^- in its $^2\Pi_{1/2}$ excited state dissociates into I^- + Br. Figure 6 shows schematic quasi-diatomic potentials for the Xe–IBr system as a function of Xe–IBr distance.[20] Two ionic potentials are shown. Surface I is the potential of Xe^+ with IBr^- in its ground electronic state. Trajectories following this surface will lead to recombination of Xe^+ with Br^-, and therefore to formation of XeBr*. Surface II involves IBr^- in an excited state and leads to formation of XeI*. Several authors have addressed the question of how surface II can be reached.[19–22] Two possible

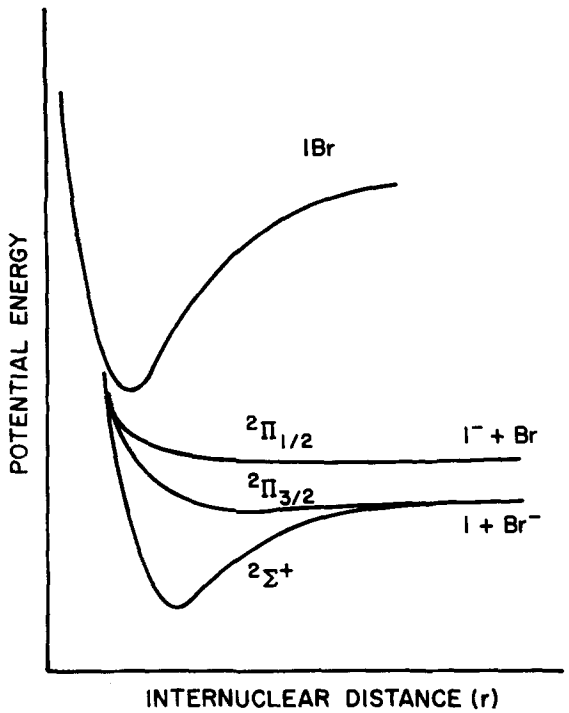

FIG. 5. Schematic potential energy diagram as function of I–Br separation for a fixed Xe–IBr distance.

processes have been suggested: (i) If the electron jump does not always take place at R_c(I), then the trajectory can continue on the neutral potential and couple with surface II at R_c(II), or (ii) the trajectories might follow surface I at long range, and then couple to surface II at short internuclear distances. We have previously observed a steric effect in reaction (1) which could be explained with either of these models.[23]

In studies of alkali metal (M) reactions with IBr and ICl, MI products were found by Kwei and Herschbach[20] and by Scholeen and Herm.[24] For fast alkali chemiionization with the same systems, Auerbach *et al.*[21] observed I^- ions at the lower collision energies. With homonuclear halogens there are also indications that the excited ionic potential surface plays a role in the reaction dynamics. In that case the excited X_2^- dissociates into $X^- + X^*$ and the reaction products are

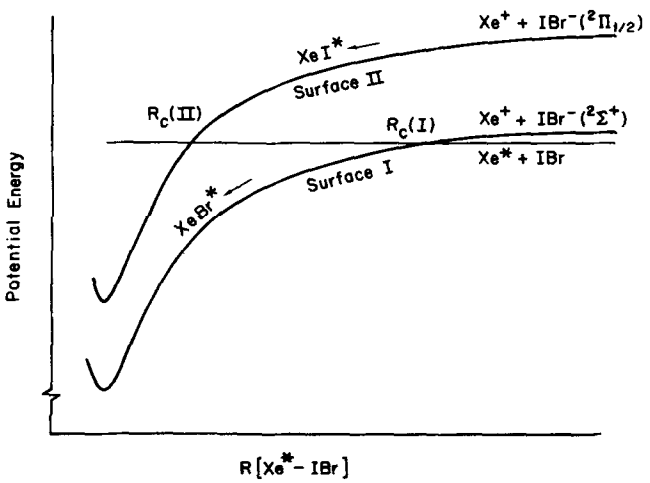

FIG. 6. Schematic potential energy diagram as a function of Xe–IBr separation for a fixed I–Br distance.

$MX + X^*$. Since the product atom is spin–orbit excited there is less energy available for vibrational excitation of the product molecule. The bimodal product velocity distribution for $K + I_2 \rightarrow KI + I$ has been interpreted to be the result of a bimodal vibrational population.[25] This is presumably due to the fact that a fraction of the trajectories follow the excited potential surface. Setser *et al.*[8–14] have studied vibrational populations of excimers from reactions of metastable rare gases with homonuclear halogens. The product excimer spectra were analyzed and there was some evidence for bimodal distributions, with the effect increasing with halogen mass. The average excimer vibrational excitation was also found to decrease with halogen mass. Both of these trends are in agreement with the trend in halogen atom ($^2P_{1/2}$–$^2P_{3/2}$) spin-orbit splitting, which increases with mass. The fraction of reactive alkali collisions which involve the excited ionic surface is estimated to be of the order of 10%.[18] For the metastable rare gas atoms (Ar*, Kr*, Xe*) reacting with ICl and IBr, Setser *et al.*[8,14] find AI* production to be of the order of 50%, significantly higher than for the alkalis. Our XeI*/XeBr* ratio of 0.40 in the present work is in good agreement with these results.

For the homonuclear halogens a fraction of the trajectories are expected to pass R_c(I) without an electron jump, since for certain approach geometries the coupling matrix element goes to zero.[2] However with the interhalogens this is not the case. Therefore, in order for trajectories not to initially follow surface I, the coupling matrix element at R_0(I) would have to be small. This would be the case when ΔV = I.P.(A*) – E.A.(XY) is small. It is conceivable that the E.A. is increased due to "prestretching" of the halogen bond, caused by the perturbation of the approaching A* atom.[26] This effect is expected to be largest at low collision velocities. With increasing velocity there would be less prestretching, and therefore fewer trajectories would pass R_c(I) and reach surface II. For Xe*/IBr this would imply an increasing fraction of XeBr* with increasing velocity, consistent with Fig. 4.

If we assume that all trajectories initially follow surface I, formation of XeI* must involve a mechanism which couples the two ionic surfaces at close range. One might consider the various Xe–IBr* potentials as possible intermediates, but this seems unlikely since formation of IBr* constitutes only 7% of the total reaction cross section.[3] Another possible mechanism is suggested by Gislason,[19] with reference to calculations by Balint-Kurti[27] for $Li + F_2$ potential surfaces. In that analogous system the excited ionic potential is degenerate with the ground state ionic potential at short range and in specific conformations. Kimura and Lacmann[28] have measured differentially scattered K^+ in $K + Br_2$, Cl_2 ion pair formation. They conclude that $K^+ + X_2^{-*}$ is formed from a *deeper* potential well than $K^+ + X_2^-$. This implies that at close range the $K^+ + X_2^{-*}$ potential is pulled down below the $K^+ + X_2^-$ potential by the approaching K^+ atom. It would then be possible for the ground state and the excited state ion pair potential to be coupled. A mechanism along these lines has been suggested by Kwei and Herschbach[19] for reactions of alkali atoms with mixed halogens. For M + IBr collisions they suggest on the

basis of MO arguments that on surface I, for small r, the electron charge is mainly on the I atom. When the IBr bond stretches, the charge of an unperturbed IBr^- would migrate to the Br atom, leading to dissociation into $I + Br^-$. However the approaching M^+ could cause the charge to remain on the I atom, leading to formation of MI. This is equivalent to saying that the approaching M^+ deforms the potentials so as to provide a coupling between surface I and surface II. A rare gas ion is much more electronegative than an alkali ion. The rare gas metastable acts as a pseudoalkali at long range, while the rare gas ion acts as a pseudohalogen at short range.[29] Therefore, a rare gas ion might be expected to perturb the potentials more strongly and keep the charge on the I atom at larger range than does an alkali ion. This would explain why the AI*/ABr* branching ratios are higher than the MI/MBr ratios. In connection with the pseudohalogen description, it should be noted that bimodal product vibrational distributions have also been observed in studies of halogen atom/halogen molecule atom transfer reactions.[30]

We have suggested above that prestretching of IBr could lead to a greater fraction of trajectories passing R_c(I) at low velocities, giving a higher XeI*/XeBr* ratio. The migration of charge with change in IBr^- internuclear distance provides an alternative "phase matching" model.[7] In this model we assume that all reactive trajectories cross to surface I at R_c(I), and that the branching ratio results from the coupling with surface II at close range. We have calculated the time t_a it takes for the $Xe^+ + IBr^-$ system after its formation at R_c(I) to reach a distance of 4 Å. Referring to Fig. 5 it is seen that the IBr^- ion starts vibrating after formation via a vertical electronic transition from IBr. The time t_a, which depends on the initial relative velocity, is indicated in Fig. 4 for zero impact parameter collisions and an assumed value R_c(I) = 6 Å. With a IBr^- vibrational period of the order of 1.6×10^{-13} s, the ion completes about one vibration at the lower velocities during t_a. This would cause the Xe^+ to arrive when the IBr^- is at the minimum vibrational amplitude, where the charge tends to be on the I atom, giving a favorable configuration for the formation of XeI*. At the higher velocities, the Xe^+ would arrive after less than a full vibration of IBr^-, giving a more favorable configuration for the formation of XeBr*. Thus a phase matching effect between the IBr^- vibrational motion and the trajectory motion could be responsible for the observed increase in the XeBr*/XeI* branching ratio at high velocities.

The above models serve mainly to illustrate the qualitative effects which are expected to control the cross sections for different reaction channels. More quantitative models would require integration over all impact parameters on accurate potential surfaces. It must be noted that different impact parameters will lead to very different trajectories, i.e., larger impact parameter trajectories will spend more time on the ionic potential surface, due to centrifugal repulsion. The approach geometry is also important. In analogy with the alkali/halogen cases,[29] the coupling may be more effective in a bent configuration than in a linear configuration.

Another question concerns the different electronic state branching ratios that we observe for Xe*/IBr as compared with the homonuclear halogens. Correlation diagrams show that formation of excimers in different electronic states involves different electronic states of the intermediate ion pair.[14,17] According to Kolts *et al.*,[14] in the case of Xe^*/Cl_2 the excimer B state correlates with $Cl_2^-(^2\Pi)$. In other words, in that case both formation of the XeBr* B state and formation of XeI* may require trajectories that proceed over surface II. Therefore, XeI* formation might be expected to compete with formation of XeBr* (B), which would explain the relatively large XeBr* C/B ratio observed in this work.

We conclude that both the present results, and the observed steric effect in the Xe*/IBr collisions reported earlier,[23] are consistent with the assumption that XeI* is formed via the $^2\Pi_{1/2}$ ionic intermediate, surface II. These experiments are inconclusive in deciding which of the two proposed mechanisms, coupling between the covalent surface and surface II, or between the ionic surfaces I and II, is dominant in XeI* formation.

ACKNOWLEDGMENT

Support of this work by the U.S. Department of Energy Office of Basic Energy Sciences (Grant DE-AMO3-76SF-00034) is gratefully acknowledged.

[1]M. Polanyi, Endeavour **8**, 3 (1949).
[2]J. Loss and A. W. Kleyn, in *Alkali Vapors*, edited by P. Davidovits and D. L. McFadden (Academic, New York, 1979).
[3]D. W. Setser, T. D. Dreiling, H. C. Brashears, and J. H. Kolts, Faraday Discuss. Chem. Soc. **67**, 255 (1979).
[4]K. T. Gillen, T. D. Gaily, and D. C. Lorents, Chem. Phys. Lett. **57**, 192 (1978).
[5]A. P. Hickman and K. T. Gillen, J. Chem. Phys. **73**, 3672 (1980).
[6]M. F. Golde, in *Gas Kinetics and Energy Transfer* (The Chemical Society, London, 1977), Vol. 2.
[7]M. S. de Vries and R. M. Martin, Chem. Phys. **80**, 157 (1983).
[8]K. Tamagake, D. W. Setser, and J. H. Kolts, J. Chem. Phys. **74**, 4286 (1981).
[9]H. L. Snyder, B. T. Smith, and R. M. Martin, Chem. Phys. **65**, 397 (1982).
[10]F. Bozso, J. T. Yates, Jr., J. Arias, H. Metiu, and R. M. Martin, J. Chem. Phys. **78**, 4256 (1983).
[11]T. P. Parr and R. M. Martin, J. Chem. Phys. **69**, 1613 (1978).
[12]P. J. Hay and T. H. Dunning, J. Chem. Phys. **69**, 2209 (1978).
[13]F. B. Dunning, T. B. Cook, W. P. West, and R. F. Stebbings, Rev. Sci. Instrum. **46**, 1072 (1975).
[14]J. H. Kolts, J. E. Velazco, and D. W. Setser, J. Chem. Phys. **71**, 1247 (1979).
[15]N. Sadeghi and D. W. Setser, Chem. Phys. Lett. **82**, 44 (1981).
[16]J. A. R. Samson, *Techniques of VUV Spectroscopy* (Wiley, New York, 1967), p. 212.
[17]C. T. Rettner and J. P. Simons, Faraday Discuss. Chem. Soc. **67**, 329 (1979).
[18]R. Grice and D. R. Herschbach, Mol. Phys. **27**, 159 (1974).
[19]E. A. Gislason, in *Alkali Halide Vapors* edited by P. Davidovits and D. L. McFadden (Academic, New York, 1979).
[20]G. H. Kwei and D. R. Herschbach, J. Chem. Phys. **51**, 1742 (1969).
[21]D. J. Auerback, M. M. Hubers, A. lP. M. Baede, and J. Los, Chem. Phys. **2**, 107 (1973).
[22]J. M. Yuan and D. M. Micha, J. Chem. Phys. **65**, 4876 (1976).
[23]M. S. de Vries, V. I. Srdanov, C. P. Hanrahan, and R. M. Martin, J. Chem. Phys. **78**, 5582 (1983).
[24]C. M. Scholeen and R. R. Herm, J. Chem. Phys. **65**, 5398 (1976).
[25]K. T. Gillen, A. M. Rulis, and R. B. Bernstein, J. Chem. Phys. **54**, 2831 (1971).
[26]J. A. Aten and J. Los, Chem. Phys. **25**, 47 (1977).
[27]G. G. Balint-Kurti, Mol. Phys. **25**, 393 (1973).
[28]M. Kimura and K. Lacmann, J. Chem. Phys. **69**, 4938 (1978).
[29]S. J. Buelow, D. R. Worsnop, and D. R. Herschbach, Faraday Discuss. Chem. Soc. **67**, 359 (1979).
[30]T. Trickl and J. Wanner, J. Chem. Phys. **78**, 6091 (1983).